

Effect of Thermal Treatments on the Yielding of Polycarbonate

E. Kontou

Department of Applied Mathematical and Physical Sciences, Section of Mechanics, National Technical University of Athens, 5 Heroes of Polytechnion, GR-15773, Athens, Greece

Received 29 June 2004; accepted 30 January 2005

DOI 10.1002/app.22077

Published online in Wiley InterScience (www.interscience.wiley.com).

ABSTRACT: Two different thermal treatments were applied to polycarbonate (PC) in terms of slow cooling (annealed samples) after a thermal treatment at a temperature above the glass-transition temperature or abrupt cooling in a liquid-nitrogen environment (quenched samples). Tensile and compression experiments were performed on the two types of samples at three different effective strain rates. A viscoplastic model based on the fundamental assumptions of the Eyring model and on a kinematic formulation, which

separated the viscoelastic and plastic strain, developed in previous works, was used to describe the yield and postyield behavior of thermally treated PC. The different thermal treatments affected the parameters of the material microstructure. A satisfactory agreement between the experimental data and calculated results was found. © 2005 Wiley Periodicals, Inc. *J Appl Polym Sci* 98: 796–805, 2005

Key words: annealing; yielding; activation energy

INTRODUCTION

A lot of work has dealt with the effect of thermal treatments on the mechanical behavior of solid polymers,^{1–10} but the molecular mechanism or physical modification occurring during these treatments is still a subject of interest. The distributed nature of the microstructural state of amorphous polymers and the way in which it is affected by thermal treatments may play important roles in determining a material's inelastic properties, such as nonlinear viscoelasticity and yielding. The changes in the mechanical properties that take place during physical aging must be attributed to structural changes within the polymer and may be eliminated via heating above the glass-transition temperature (T_g) or during the postyield stage. The interpretation of the origin of these changes is usually based on the estimation and distribution of the free volume, on enthalpy changes, and on the study of chain conformations.

On the other hand, the yielding of glassy polymers has over the last 2 decades been the subject of a number of works and is still a matter of great interest.^{11–16} Two main categories of theories, one based on viscous flow and the other simulating plastic deformation in metals, are usually considered to describe the inelastic behavior of glassy polymers. The deformation mechanism of the glassy state, which is a su-

percooled liquid, can be considered a molecular process (related to the main-chain segmental mobility) that mainly occurs above T_g . Such a large-scale diffusion motion is generally inconsistent with intrinsic strain softening and subsequent strain localization. However, under the combined influence of stress and thermal energy kT , where k is the Boltzmann constant and T is the temperature, the plastic strain rate is determined with the Eyring concept.¹⁷ A lot of treatments of yielding in glassy polymers have been based on this concept. The history dependence of the yield stress at a constant strain rate and temperature indicates that the activation energy, which is involved in the Eyring equation, grows during physical aging. Treatments just below T_g result in volume contraction and enthalpic relaxation, leading to an increase in the polymer yield stress. Treatments far below T_g instead reduce the polymer's capacity for low-stress anelastic deformation.⁷

According to the earlier treatments, yield takes place by a liquidlike flow, when adiabatic heating raises the temperature locally, or during the deformation procedure, in which an increase in the free volume results in the shifting of T_g to the deformation temperature.⁴

Although these concepts have been doubted many times,^{2,3,18} a strong association between the yield and free volume has been historically established.

On the other hand, uniaxial compression leads to less free volume, whereas in all cases, the relative changes in the free volume are about five times greater than relative changes in the macroscopic volume. Hasan and Boyce⁵ found that the free volume in un-

Correspondence to: E. Kontou (ekontou@central.ntua.gr).

strained poly(methyl methacrylate) (PMMA) is reduced by physical aging, but it is independent of the thermal history beyond the yield point.

This is relevant to the increase in the yield stress and the independence of large strain flow stress after aging.

The effect of thermal or physical aging in increasing the yield stress of glassy polymers was first observed by Horsley¹⁹ with poly(vinyl chloride) (PVC) and in a number of later works.^{20–22} The results of Struik²¹ for PVC provided important information about the physical aging process, including the increase in the yield stress with storage at a constant temperature. The reversibility of the aging process was also demonstrated.

Positron annihilation lifetime spectroscopy (PALS) has proved to be extremely useful in studying the free volume and free volume distribution and how they are affected by physical aging. Results reported for polycarbonate (PC) reveal that the consequences of physical aging and temperature changes are qualitatively different: reducing the temperature results in a decrease of the hole size, whereas as aging proceeds, the number of holes decreases, with apparently little reduction in the hole size. There is a strong association between the yield and free volume, and in recent years, PALS has been used to probe the free volume in liquid, glassy, and semicrystalline polymers.⁴

Hasan et al.⁶ observed an increase in the free volume with compressive straining beyond the yield, using PALS on annealed and quenched specimens of PMMA. The increase in the free volume upon straining was accompanied by strain softening. Before deformation, the annealed sample was found to have a lower free volume content than the quenched sample. After 30% deformation, the two materials exhibited the same free volume content, which was higher than that observed in the undeformed samples. The actual changes in the macroscopic volume even during prolonged aging are often small and seldom exceed 0.2%.

In this work, the effects of the thermal history (annealing and quenching) on the mechanical properties (tensile and compressive yield and postyield behavior) of a representative glassy polymer PC were studied.

Thermal treatments are associated with the distributed nature of the material state or, more specifically, with the free volume distribution changes or localized regions of large strain inhomogeneities, at which irreversible transformations take place, during deformation procedures. On the basis of previous works,^{16,23} the rate of plastic deformation follows a normal distribution function; therefore, it could accordingly be changed by the material thermal history. Furthermore, yielding was considered a thermally activated rate process. All these assumptions were combined with a typical constitutive equation of nonlinear viscoelastic-

ity, and it was shown that model parameters related to the material state distribution were affected by the thermal history. The calculated results were found to be close to the experimental ones, thus revealing that our analysis based on the macroscopic material behavior results in useful information about the material state at a microscopic level.

EXPERIMENTAL

The tested material was a commercial grade of PC called Lexan, a product of General Electric Plastics, and it was provided in a plate form. The same grade was used for both tensile and compression experiments. Two different heat treatments were applied to the studied material. All samples were annealed at 160°C, which is a temperature above T_g (140°C), for 4 h, and they were subsequently either slowly cooled at room temperature (annealed samples) or imposed in liquid nitrogen (quenched samples).

Tensile and compressive experiments were performed at room temperature at various crosshead speeds, namely, 0.1, 1, and 10 mm/min, which coincided with a total effective strain rates of 5.55×10^{-5} , 5.55×10^{-4} , and $5.55 \times 10^{-3} \text{ s}^{-1}$, respectively, for tensile specimens with a 30-mm gauge length. The specimens for compression were cylindrical with a mean diameter of 10 mm and a height of 20 mm. Therefore, the corresponding effective strain rates in compression were 8.33×10^{-5} , 8.33×10^{-4} , and $8.33 \times 10^{-3} \text{ s}^{-1}$.

The experiments were carried out with an Instron type 1121 tester (Instron Ltd., Buckinghamshire, UK), whereas the longitudinal strain was measured with a noncontact method through the use of a laser extensometer described in detail elsewhere.²⁴ According to this method, a laser beam scans a tape pattern code applied to the specimen, namely, a number of white stripes on a dark background. During both the tensile and compression tests, the load and strain were recorded simultaneously, with the data acquisition being performed by a computerized system. This experimental technique has the advantage of giving a detailed description of the strain and the corresponding strain rates along the gauge length of the tested material.

CONSTITUTIVE ANALYSIS

Many treatments of yielding in glassy polymers are based on the Eyring model, in which the macroscopic strain rate is determined by a combination of applied stress and thermal energy kT .¹⁷ According to the theory of thermal activation, as proposed by Eyring (and further used by Bauwens-Crowet et al.²⁵ to describe creep experiments), the macroscopic strain rate takes the following form:

$$\dot{\varepsilon} = \dot{A} \exp\left(\frac{-\Delta H + v\sigma}{kT}\right) = \dot{B} \exp\left(\frac{v\sigma}{kT}\right) \quad (1)$$

where σ is the stress, ΔH is the activation energy, v is the activation volume, and the pre-exponential factors are constants.

According to this formalism, $\frac{d\sigma_y}{d \ln \dot{\varepsilon}}$ is a constant, where σ_y is the yield stress, and leads to the calculation of v and constant \dot{B} . v expresses the volume of polymer segments needed to move as a whole for plastic yielding to occur. Yielding occurs when the product of the relaxation time τ and the applied strain rate $\dot{\varepsilon}$ reaches a constant value close to unity:¹⁷

$$\dot{\varepsilon}\tau \equiv 1 \quad (2)$$

Therefore, through the combination of eqs. (1) and (2), τ is expressed as a stress-dependent function:

$$\tau = \tau_0 \exp\left[\frac{-(\sigma - \sigma_{\text{int}})v}{kT}\right] \quad (3)$$

The term σ_{int} has been introduced as an internal variable, and it defines the deformation resistance that the material has to overcome because of the molecular alignment occurring after yielding and stress overshooting. This molecular alignment results in a change in the configurational entropy of the system.

σ_{int} introduced in ref. 26, is given by

$$\sigma_{\text{int}} = C_R \frac{\sqrt{N}}{3} \left[\lambda_i L^{-1} \frac{\lambda_i}{\sqrt{N}} - \left(\frac{1}{3}\right)^3 \sum_{j=1}^3 \lambda_j L^{-1} \frac{\lambda_j}{\sqrt{N}} \right] \quad (4)$$

where λ_i is the stretch ratio; λ_j is the stretch ratio in the other principal direction, which is defined by the assumption of isovolume deformation during yielding; C_R is the rubbery modulus; and L^{-1} is the inverse Langevin approximation. N is the number of rigid chain links between physical molecular chain entanglements.

Assuming that the stress-strain behavior of the glassy state follows a thermally activated viscoelastic path at small strains, the well-known constitutive equation of viscoelasticity can be used:

$$\sigma(t) = \int_0^t E_0 \exp(\xi - \xi') \frac{d\varepsilon}{d\lambda} d\lambda \quad (5)$$

E_0 is the apparent modulus, equal to 2300 MPa, and ξ and ξ' represent the reduced time:²⁷

$$\xi = \int_0^t \frac{dt'}{a[\sigma(t')]} \quad \xi' = \int_0^\lambda \frac{dt'}{a[\sigma(t')]} \quad (6)$$

The shift factor a is the ratio τ_r/τ , where τ_r is the relaxation time in a reference state of deformation and τ is the relaxation time in every state of deformation.

To describe the yield and postyield behavior after the initial viscoelastic path, we assume that at this stage the plastic path prevails.^{16,23} A kinematic formulation that separates the elastic (viscoelastic) strain from the plastic strain, developed by Rubin,²⁸ has been successfully applied in previous works^{16,23} and is now used here. For a uniaxial deformation, the time evolution of the stretch ratio \dot{a}_m of the viscoelastic deformation is given by¹⁶

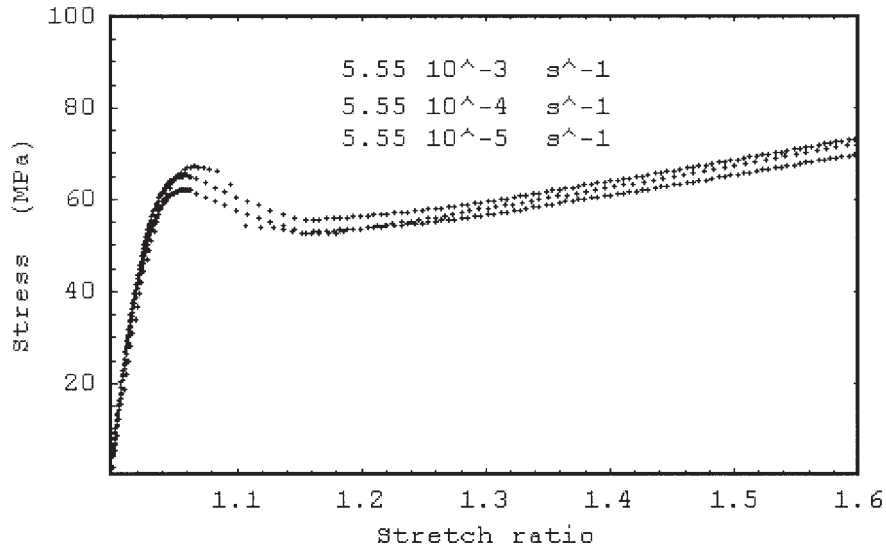
$$\frac{\dot{a}_m}{a_m} = f(a_m) \left[\frac{\dot{a}}{a} - \frac{\dot{\Gamma}_p}{18g} g(a_m) \right] \quad (7)$$

where $f(a_m)$ and $g(a_m)$ are specific functions of the elastic strain a_m , \dot{a} is the imposed strain rate, a is the stretch ratio, and $a_m(0)$ is equal to 1. The quantity $\dot{\Gamma}_p$, expressing the rate of plastic deformation, has been modeled in previous works,^{16,23} in which it has been assumed that during deformation, strain is accumulated in specific regions. This accumulation takes place around a large number of defects randomly distributed into the deformed material. It is reasonable to assume that these defects are related to regions of extra free volume. The total applied deformation will consequently be distributed inhomogeneously around these regions. When the distributed elastic energy around each region reaches a critical value, a nonreversible transition takes place, denoting the emergence of plastic deformation. If each one of these transitions proceeds at a certain rate, then the macroscopic plastic deformation will occur with a rate proportional to the number of simultaneously appearing localized transformations. Assuming that the strain accumulated around the i -region follows a normal Gaussian distribution with a mean equivalent strain $\bar{\mu}$ and a standard deviation s , then the distribution density function with the equivalent strain $\bar{\varepsilon}_i$ as a variable is given by

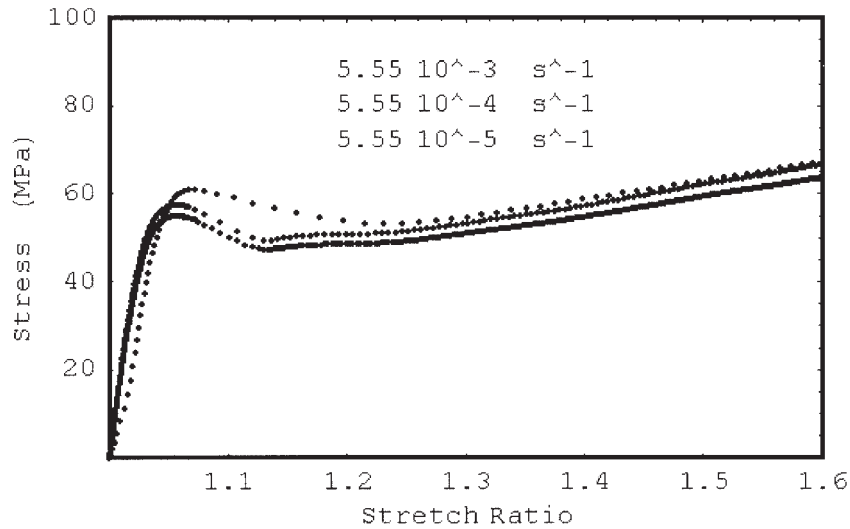
$$f(\bar{\varepsilon}_i) = \frac{1}{s\sqrt{2\pi}} \exp\left[-\frac{1}{2}\left(\frac{\bar{\varepsilon}_i - \bar{\mu}}{s}\right)^2\right] \quad (8)$$

The fraction of plastic transformations that have achieved a nonreversible state is given by the probability (P):

$$P = \frac{1}{s\sqrt{2\pi}} \int_0^\varepsilon e^{-\frac{1}{2}\left(\frac{\bar{\varepsilon}_i - \bar{\mu}}{s}\right)^2} \times d\bar{\varepsilon}_i \quad (9)$$



(a)



(b)

Figure 1 Experimental tensile stress/stretch-ratio curves for (a) annealed and (b) quenched Lexan at three different effective strain rates.

Consequently, the rate of plastic deformation $\dot{\Gamma}_p$ is and then proportional to P :

$$\dot{\Gamma}_p = \dot{k}P \tag{10}$$

where \dot{k} can be estimated from the boundary condition, according to which at the yield point the equivalent strain $\tilde{\epsilon}$ is equal to the mean value $\tilde{\mu}$, and the rate of plastic deformation $\dot{\Gamma}_p^y$ is equal to the applied effective strain rate $\dot{\tilde{\epsilon}}$. Then, because the normal distribution function is symmetric, it becomes equal to $1/2$. Therefore, we obtain

$$\dot{\Gamma}_p^y = \dot{\tilde{\epsilon}} = \dot{k} \frac{1}{s\sqrt{2\pi}} \int_0^{\tilde{\mu}} \exp\left[-\frac{1}{2}\left(\frac{\tilde{\epsilon}_i - \tilde{\mu}}{s}\right)^2\right] d\tilde{\epsilon}_i = \dot{k} \frac{1}{2} \tag{11}$$

$$\dot{\Gamma}_p = \frac{2\dot{\tilde{\epsilon}}}{s\sqrt{2\pi}} \int_0^{\tilde{\epsilon}} \exp\left[-\frac{1}{2}\left(\frac{\tilde{\epsilon}_i - \tilde{\mu}}{s}\right)^2\right] d\tilde{\epsilon}_i \tag{12}$$

RESULTS AND DISCUSSION

According to the experimental method applied for the deformation measurement, a detailed approximation of the deformation distribution along the specimen gauge length can be obtained. Because of the inhomogeneous deformation exhibited by the materials, a localized zone appears, having a magnitude of strain much higher than that of the other zones of the spec-

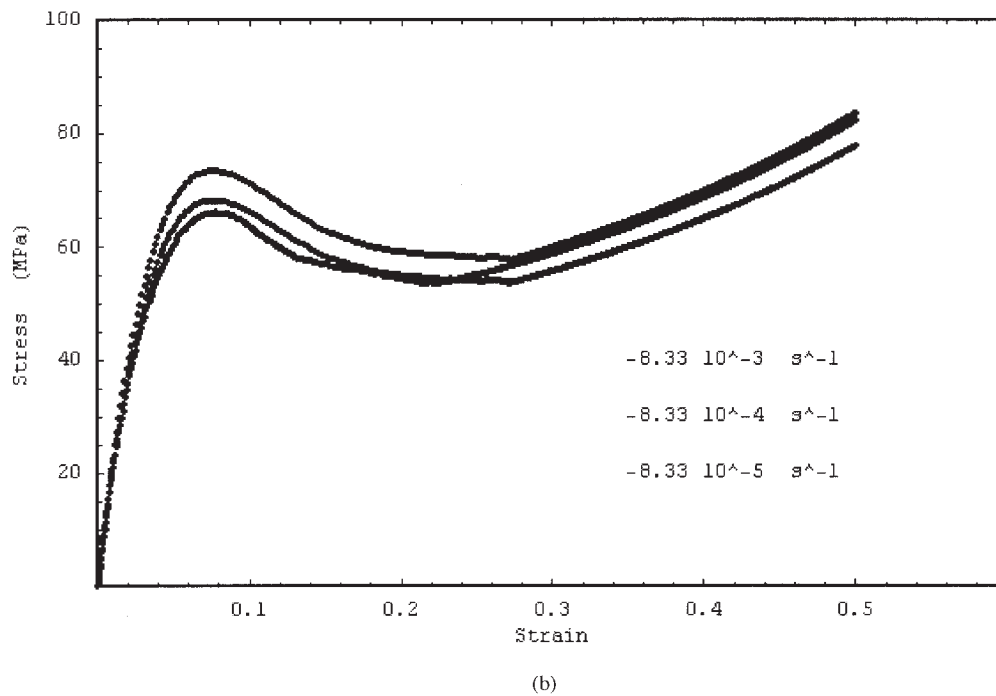
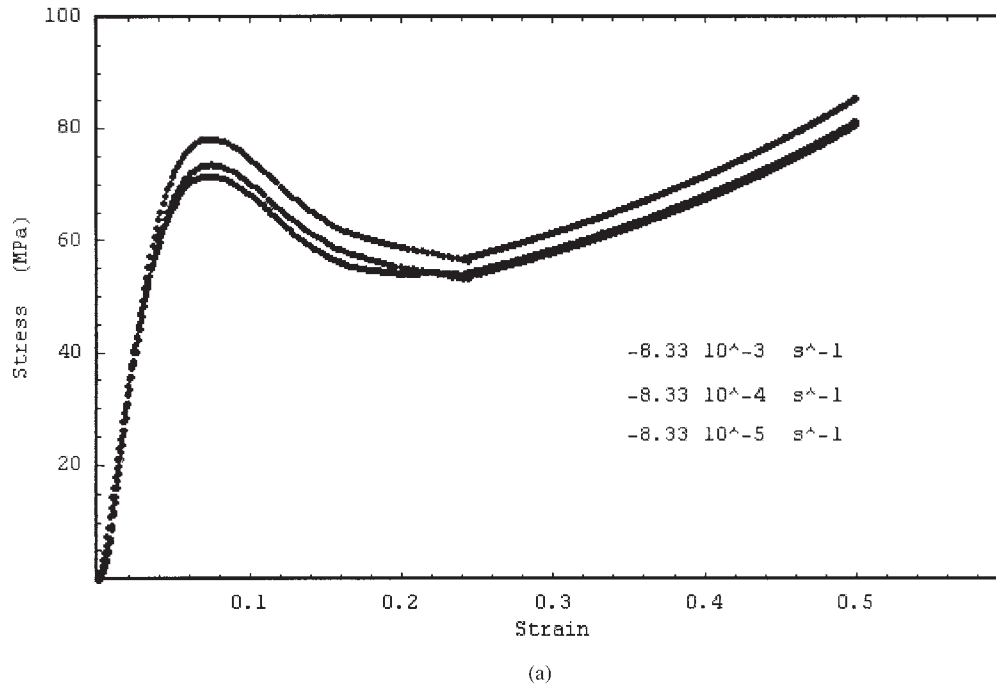


Figure 2 Experimental compression stress–strain curves for (a) annealed and (b) quenched Lexan at three different effective strain rates.

imen's gauge length. Then, the true stress–strain curves can be constructed, referring to the deformation of that specific zone, in terms of the expression, $\sigma = \sigma_0 (1 + e)$, assuming isovolume conditions, where σ is the true stress, σ_0 is the nominal stress, and e is the strain of the specific reference zone. The experimental stress/stretch-ratio curves of annealed and quenched samples for tension are presented in Figure 1(a,b) at

three different strain rates. The corresponding curves for the compression experiments are shown in Figure 2(a,b). The quenching procedure leads to lower yield stress,⁴ whereas all figures exhibit the typical mechanical response of initial viscoelastic behavior, yield stress, strain softening, and strain hardening. The rate effect is also obvious, and this fact can be attributed to the thermally activated process during inelastic defor-

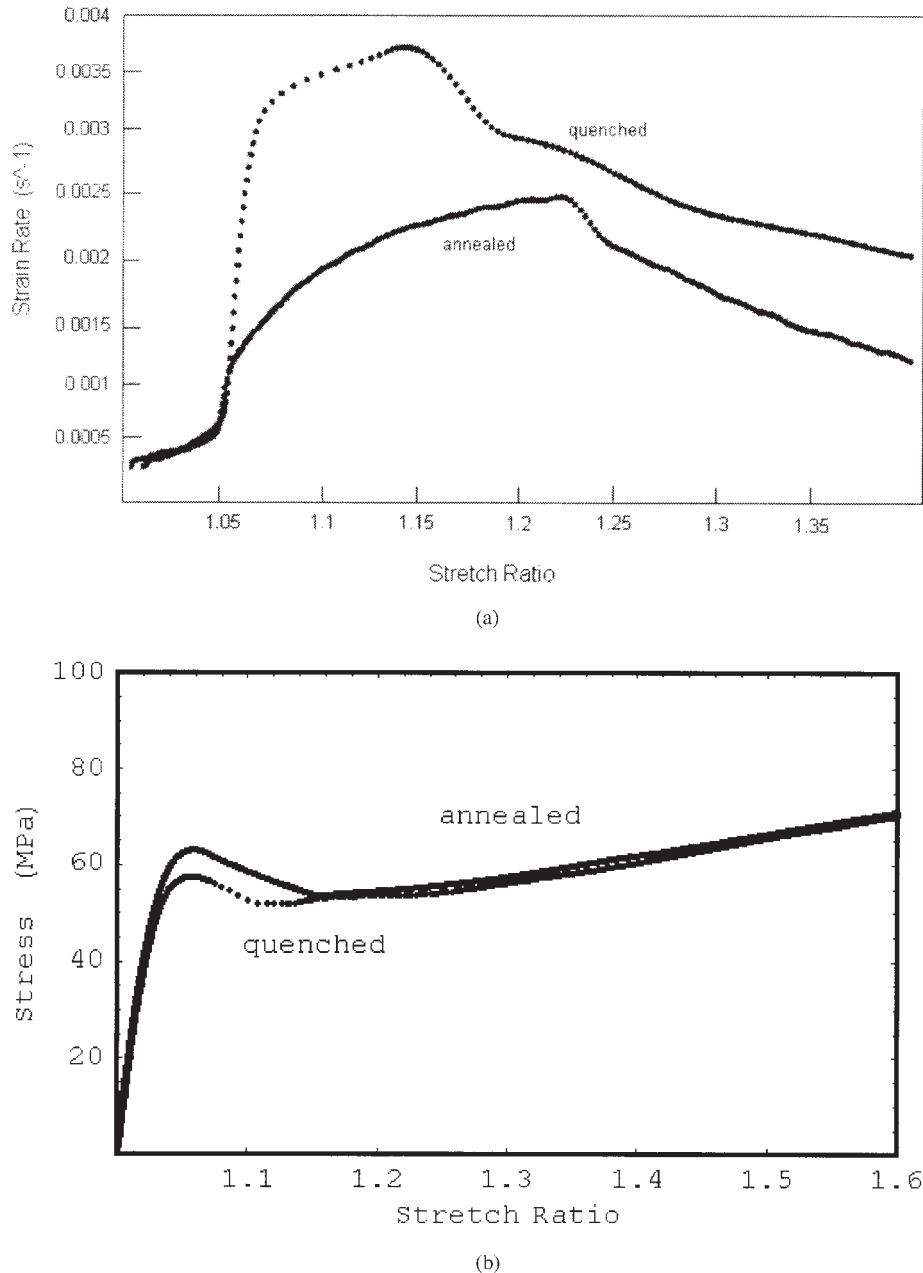


Figure 3 (a) Experimental strain rate versus the stretch ratio of the zone with maximum strain for annealed and quenched Lexan at an effective strain rate of $5.55 \times 10^{-4} s^{-1}$ and (b) experimental tensile stress/stretch-ratio curves for annealed and quenched Lexan at an effective strain rate of $5.55 \times 10^{-4} s^{-1}$.

mation of glassy polymers. From the experimental data available, the localized strain rate as a function of the strain expressed in a stretch ratio for the zone of maximum deformation can also be evaluated via

$$\dot{\epsilon} = \frac{de}{(1+e)dt}$$

A representative plot of the strain rate is presented in Figure 3(a), obtained from tensile experiments for an effective strain rate equal to $5.55 \times 10^{-4} s^{-1}$. The strain-rate data are plotted for annealed and quenched samples. The two curves exhibit the same features.

Initially, they coincide at the onset of yielding when the strain rate of this localized region becomes equal to the imposed effective strain rate. Hereafter, the strain rate of the quenched sample exhibits a rapid increment up to an almost constant value, remaining at this value up to a stretch ratio of 1.15. During this stage, necking and neck propagation are completed in the boundaries of this zone, and this leads to strain softening. Then, the decrement of the strain rate is strong evidence of the onset of strain hardening. The annealed sample exhibits a similar increment, but it

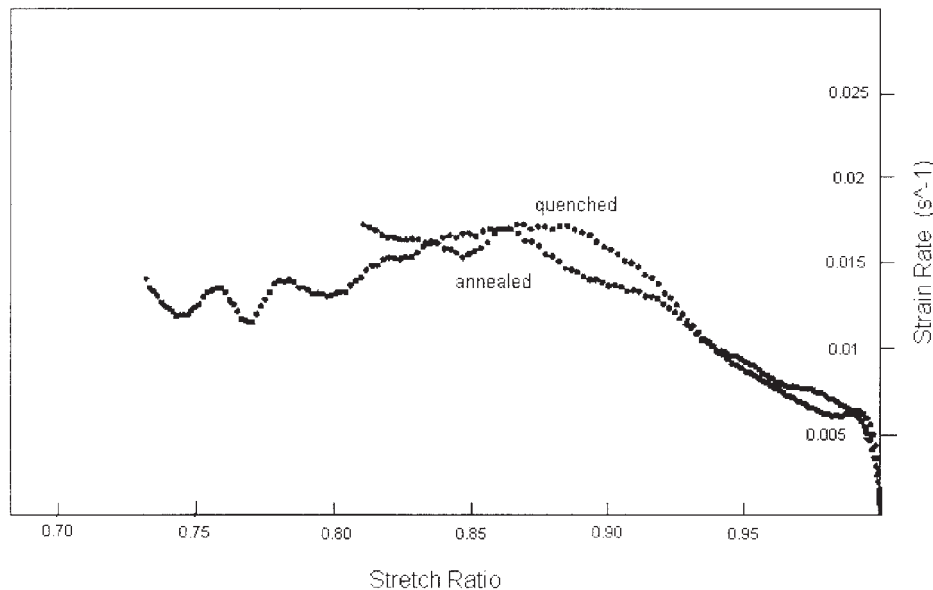


Figure 4 Experimental strain rate versus the stretch ratio of the zone with maximum strain for annealed and quenched Lexan at an effective strain rate of $-8.33 \times 10^{-3} \text{ s}^{-1}$.

achieves a much lower plateau value, which continues up to a stretch ratio of 1.23. The rapid increment of the strain rate in this localized zone, for both treatments, is strongly related to the appearance of strain softening. These remarks are consistent with the stress-strain curves of the materials, which are replotted for reasons of clarity in Figure 3(b). At large deformations, they follow the same trend, and this fact has also been observed in previous works.⁴⁻⁶ The quenched material [Fig. 3(b)] exhibits a lower percentage of strain softening, whereas its strain hardening starts earlier than that of the annealed sample. This fact is reflected in Figure 3(a), in which the decrement of the strain rate also starts earlier. These observations lead to the conclusion that the different thermal treatments imposed on the materials cause significant structural changes, as will also be discussed in the following. Regarding the compression experimental results, no large strain inhomogeneity was detected in either annealed or quenched samples; therefore, the corresponding curves of the strain rate versus the strain for

the reference zone were similar, as shown in Figure 4 for an effective strain rate of $8.33 \times 10^{-3} \text{ s}^{-1}$.

With the application of eq. (1), the experimental data of Figures 1 and 2 were used to plot the yield stress as a function of the logarithmic rate of deformation. The slope of the obtained straight line leads to the calculation of the quantity v/kT , as well as the calculation of v , for the slowly cooled and quenched materials for both types of experiments. For the tensile experiments, a lower value of the volume has been found for quenched samples, whereas for compressive tests, a slightly higher volume has been estimated. These values are presented in Table I. The intersection of these lines also gives an estimation of constant \dot{B} of eq. (1), and it is presented in Table I in terms of the pre-exponential factor τ_0 of eq. (3).

As shown in Table I, v , which is approximately 3097 \AA^3 for annealed samples, exhibits a decrement of the order of 14% for the quenched samples in the tension experiments, whereas in compression, a slight incre-

TABLE I
Model Parameter Values

	v/kT (MPa ⁻¹)	v (Å ³)	$\bar{\mu}$	s	τ_0 (s)	C_R (MPa)	N
Tension							
Annealed	0.766	3097	0.03	0.009	7.44×10^{24}	15	15
Quenched	0.657	2660	0.028	0.015	7.95×10^{19}	20	15
Compression							
Annealed	0.46	1860	0.04	0.015	8.29×10^{17}	5	20
Quenched	0.51	2070	0.03	0.025	3.9×10^{18}	5	20

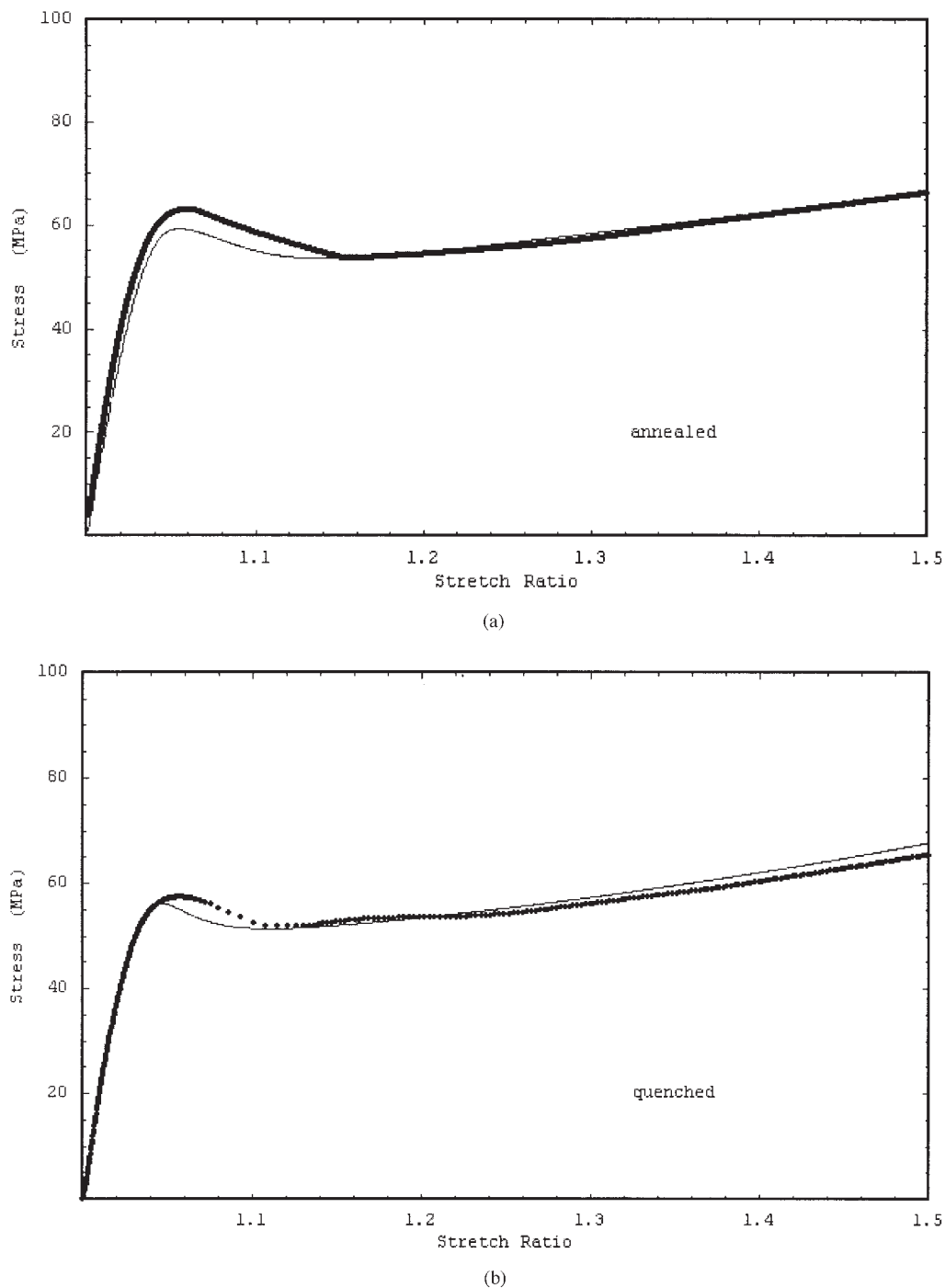


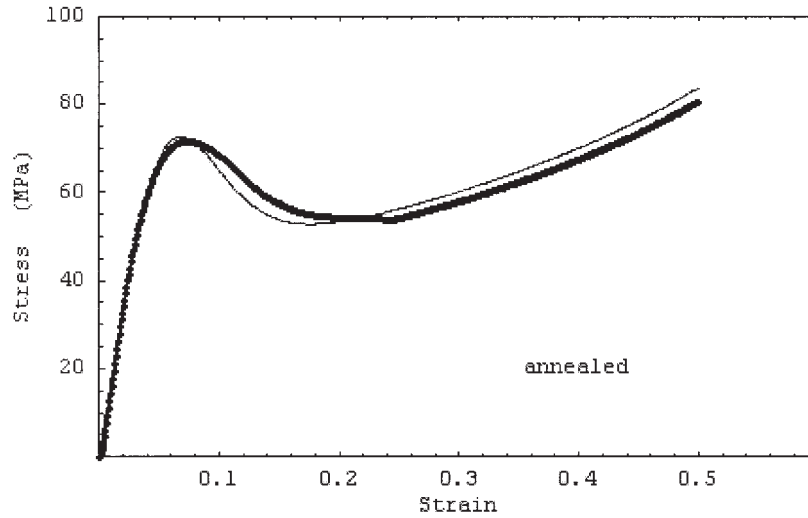
Figure 5 Tensile stress/stretch-ratio curves for (a) annealed and (b) quenched Lexan at an effective strain rate of $5.55 \times 10^{-4} \text{ s}^{-1}$. The points show experimental data, and the lines show calculated results.

ment of ν of the order of 11% can be observed from 1860 to 2070 \AA^3 . In our analysis, the activation volume acquires a broader meaning, involving the concepts of holes, defects, free volume sites, and molecular segments that rearrange cooperatively for plastic flow to occur.

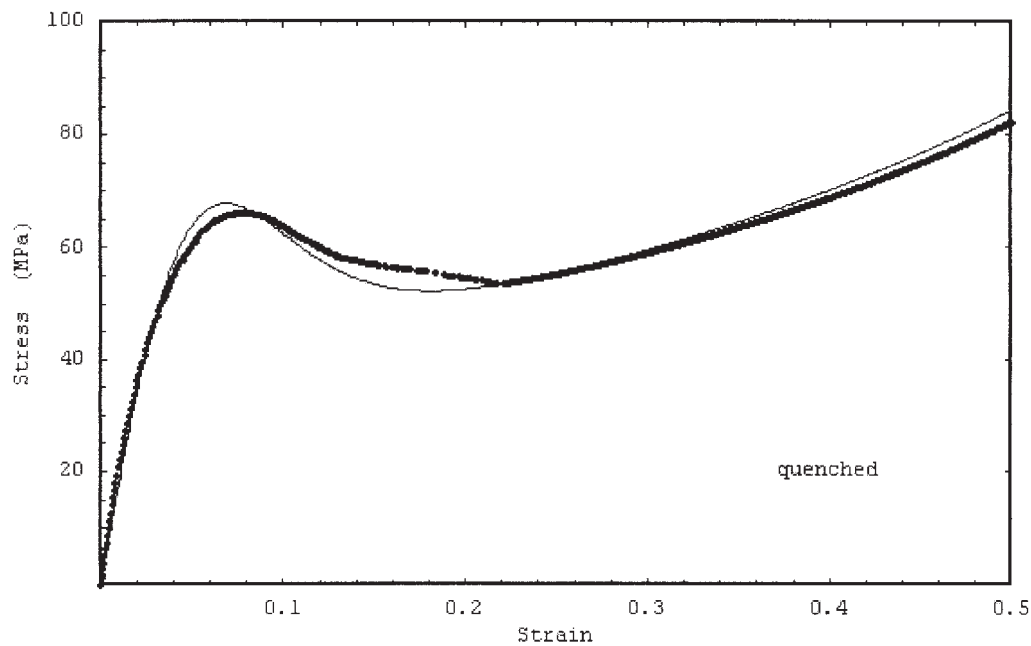
Regarding compression, the observed increment is consistent with the work by Hasan and Boyce,⁵ who obtained an analogous effect with the PALS method.

As far as tension is concerned, the higher value of the activation volume is consistent with earlier results²⁹ in which the free volume increased with the applied stress, despite the large reduction in the overall volume, and this gave rise to increased mobility.

With the kinematic formulation of eq. (7), the viscoelastic strain could be calculated by step integration, and with the combination of eqs. (3–6) and (12), the stress-strain response of all the material samples



(a)



(b)

Figure 6 Compressive stress–strain curves for (a) annealed and (b) quenched Lexan at an effective strain rate of $-8.33 \times 10^{-3} \text{ s}^{-1}$. The points show experimental data, and the lines show calculated results.

could be described, whereas the strain softening was predicted in a self-consistent manner. Integration in eq. (12) was performed numerically with small time steps until a high convergence was obtained.³⁰ The values of the required parameters are listed in Table I.

Parameters C_R and N were fitted for the best approximation. Moreover, the mean value of the probability density function was 0.03 for annealed samples and 0.028 for quenched samples. These values are close to the experimentally observed yield strain, s , which is a fitting parameter, in combination with the other model parameters describes with good accuracy the experimental data, and it was found to be 0.009 for

the annealed samples and 0.015 for the quenched samples. Assuming that the distribution function of the rate of plastic deformation reflects the distribution of extra free volume sites, we conclude that the free volume distribution is sensitive to the thermal prehistory. The annealing treatment is related to a narrower distribution of the free volume, whereas the quenching procedure causes the creation of larger free volume regions and consequently broader free volume distribution. The theoretical results, in comparison with the experimental data, for the two thermal treatments examined are shown in Figures 5(a,b) for the tensile tests at a representative strain rate of 5.55

$\times 10^{-5} \text{ s}^{-1}$ and in Figures 6(a,b) for the compression tests at a strain rate of $8.33 \times 10^{-5} \text{ s}^{-1}$. A good approximation has been found for the entire shape of the experimental curves.

CONCLUSIONS

The yield behavior of PC in tension and compression at various strain rates was studied experimentally and was analyzed in terms of the nonlinear viscoelasticity, with yielding assumed to be a thermally activated rate process. A kinematic formulation separating the viscoelastic strain from the plastic strain was used. The functional form of the rate of plastic deformation, introduced elsewhere, was correlated with the free volume distribution, and it was further found that the effect of the material thermal prehistory may be related to the distributed nature of the free volume. Two different thermal treatments (annealing and quenching) were applied to the material, and model parameters correlating material microstructural changes with the effects of the thermal treatments were accordingly calculated. A satisfactory agreement between the experimental data and calculated results was found.

References

1. Bowden, P. B. In *The Physics of Glassy Polymers*; Haward, R. N.; Wiley: New York, 1973; Chapter 5.
2. Struik, L. C. E. *J Non Cryst Solids* 1991, 131, 395.
3. Crist, B. In *Materials Science and Technology*; Thomas, E. L., Ed.; VCH: New York, 1993; Vol. 12, Chapter 10.
4. Haward, R. N.; Young, R. J. *The Physics of Glassy Polymers*, 2nd ed.; Chapman & Hall: London, 1997.
5. Hasan, O. A.; Boyce, M. C. *Polym Sci Eng* 1995, 35, 331.
6. Hasan, O. A.; Boyce, M. C.; Li, X. S.; Berko, S. *J Polym Sci Part B: Polym Phys* 1993, 31, 185.
7. Heymans, N.; Van Rossum, S. *J Mater Sci* 2002, 37, 4273.
8. Govaert, L. E.; van Melick, H. G. H.; Meijer, H. E. H. *Polymer* 2001, 42, 1271.
9. van Melick, H. G. H.; Govaert, L. E.; Meijer, H. E. H. *Polymer* 2003, 44, 3579.
10. van Melick, H. G. H.; Govaert, L. E.; Baas, B.; Nauta, W. J.; Meijer, H. E. H. *Polymer* 2003, 44, 1171.
11. Boyce, M. C.; Parks, M.; Argon, A. S. *Mech Mater* 1988, 7, 15.
12. Wu, J. J.; Buckley, C. P. *J Polym Sci Part B: Polym Phys* 2004, 42, 2027.
13. Boyce, M. C.; Arruda, E. M. *Polym Eng Sci* 1990, 30, 1288.
14. Buckley, C. P.; Jones, D. C. *Polymer* 1995, 36, 3301.
15. Govaert, L. E.; Timermans, P. H. M.; Brekelmans, W. A. M. *J Eng Mater Technol* 2000, 122, 177.
16. Spathis, G.; Kontou, E. *J Appl Polym Sci* 1999, 71, 2007.
17. Eyring, H. *J Chem Phys* 1936, 4, 283.
18. Oleynik, E. F. *High Performance Polymers*; Hanser: New York, 1991.
19. Horsley, R. A. *Plastics Progress*; Illife and Sons: London, 1958; p 77.
20. Golden, J. H.; Hammant, B. L.; Hazell, E. A. *J Appl Polym Sci* 1967, 11, 1571.
21. Struik, L. C. E. *The Physical Aging of Amorphous Polymers and Other Materials*; Elsevier: New York, 1978.
22. Ruan, M. Y.; Moaddel, H.; Jamieson, A. M. *Macromolecules* 1992, 25, 2407.
23. Spathis, G.; Kontou, E. *Polym Eng Sci* 2001, 41, 1337.
24. Kontou, E.; Farasoglou, P. *J Mater Sci* 1998, 33, 147.
25. Bauwens-Crowet, C.; Bauwens, J. C.; Homes, G. *J Mater Sci A* 1969, 2, 735.
26. Wang, M. C.; Guth, E. J. *J Chem Phys* 1952, 20, 1144.
27. Ward, I. M. *Mechanical Properties of Solid Polymers*, 2nd ed.; Wiley: Chichester, England, 1990.
28. Rubin, M. B. *Int J Solids Struct* 1994, 31, 2615.
29. Muller, J.; Wendorff, J. H. *J Polym Sci Part B: Polym Phys* 1988, 26, 421.
30. Wolfram, S. *The Mathematica Book*, 4th ed.; Wolfram Media/Cambridge University Press: Cambridge, England, 1999.